Articles

Synthesis and Properties of 2,3,6,7-Tetrakis(alkoxymethyl)tetrathiafulvalenes[1]

Marye Anne Fox* and Horng-long Pan

Department of Chemistry and Biochemistry, University of Texas at Austin, Austin, Texas 78712

Received May 3, 1994[⊗]

A family of newly prepared tetrakis(alkoxymethyl)-substituted tetrathiafulvalene (TTF) derivatives **1** show melting point behavior typical for increasing length of their flexible alkyl chains and molecular weights. No evidence for the formation of a stable liquid crystalline mesophase was found. The X-ray crystal structure of **1** (n = 7) shows it to have a flat central core. Its anodic reactivity is entirely parallel to that of tetrathiafulvalene itself. The dark conductivity of a thin film of **1** (n = 7) is sensitive to temperature, with dark conductivity being enhanced at higher temperatures by as much as 5 orders of magnitude from the level observed in previously studied TTFs. Short-circuit photocurrent is observed in a symmetrical ITO sandwich cell containing a thin layer of **1** (n = 7): in such a cell, charge can be separated under bias and maintained for at least 8 h.

Introduction

Since Cowan and co-workers' first preparation of a highly conducting 1:1 complex between tetrathiafulvalene (TTF) and the electron acceptor tetracyano-*p*-quinodimethane (TCNQ),[2] charge transfer salts of TTF have attracted widespread interest because of their quasi-metallic electrical properties.[2-5] Because of their excellent conductivities, these charge transfer complexes (CTC) have many important technological applications, e.g., as electrochromic displays or electron beam lithographic resists.[6] Many methods for the preparation of TTF derivatives and their charge transfer complexes are available,[7,8] including the synthesis of several mono- and difunctionalized tetrathiafulvalenes[9-11] and of one tetrakis(thioalkyl)-substituted derivative,[14] as well as the synthesis of various polymers containing TTF-units.[12,13]

The primary features accounting for the interest in TTF and its derivatives follow from their molecular crystal structures and conductivities. For example, Saito et al.[14] found a conductivity (up to 10^{-5} Ω^{-1} cm^{-1}) in a tetrakis(thioalkyl)tetrathiafulvalene (TTF(SC_nH_{2n+1})$_4$, n = 1–18) that is several orders of magnitude higher than that in the unsubstituted parent. Furthermore, the observed conductivity increased with the lengths of the appended alkyl chains. This observation is counterintuitive, because alkyl chains are usually good insulators because of their low dielectric constants.

We now report the synthesis and characterization of a family of tetrakis(alkoxymethyl)-substituted TTFs **1** and a tetrakis(heptanoate ester)substituted TTF **2** which we hoped might exhibit interesting macroscopic properties by virtue of their improved intermolecular sulfur–sulfur

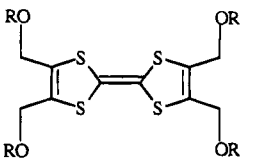

1 R = C_nH_{2n+1}, n = 1, 3, 5, 6, 7, 8, 10, 12, 14

2 R = COC_6H_{13}

atomic contacts[14-17] and might provide a test of the generality of the effect of alkyl substitution on structure and electronic properties. Included here are summaries of the X-ray structures, absorption spectra, and conductivities of selected members of this family, as well as a description of the weak short-circuit photocurrents and charge-separation under bias observed upon irradiation

⊗ Abstract published in *Advance ACS Abstracts,* October 1, 1994.

(1) Preliminary presentations of portions of this work were made at two scientific meetings: (a) Fox, M. A.; Pan, H.-L. *Photochemical Processes in Organized Molecular Systems* (Proc. Memorial Conf. for the Late Prof. Shigeo Tazuke, Yokohama, Japan, 22–24 Sept, 1990); Honda, K., Ed.; North Holland Publishers: Amsterdam, 1991; p 359. (b) Fox, M. A.; Pan, H.-L. *Proc. Soc. Photo-Opt. Instrum. Eng.* **1991**, *1436*, 2.

(2) Ferraris, J.; Cowan, D. O.; Walatka, V.; Perlstein, J. H. *J. Am. Chem. Soc.* **1973**, *95*, 948.

(3) (a) Garito, A. F.; Heeger, A. J. *Acc. Chem. Res.* **1974**, *7*, 232. (b) Tanner, D. B.; Jacobson, C. S.; Garito, A. F.; Heeger, A. J. *Phys. Rev. Lett.* **1974**, *32*, 1301.

(4) Becker, J. Y.; Bernstein, J.; Bittner, S.; Shaik, S. S. *Pure Appl. Chem.* **1990**, *62*, 467.

(5) Torrance, J. B. *Acc. Chem. Res.* **1979**, *12*, 7.

(6) Engler, E. M.; Tomkiewicz, Y.; Kuptsis, J. D.; Schad, R. G.; Patel, V. V.; Hatzakis, M. *Polymer Materials for Electronic Application*; Feit, E. D., Ed.; ACS Symposium Series, American Chemical Society; Washington, D.C., 1982.

(7) Krief, A. *Tetrahedron* **1986**, *42*, 1209.

(8) Narita, M.; Pittman, C. U. *Synthesis* **1976**, 489.

(9) Melby, L. R.; Hartzler, H. D.; Sheppard, W. A. *J. Org. Chem* **1974**, *39*, 2456.

(10) Pittman, C. U.; Narita, M.; Liang, Y. F. *J. Org. Chem.* **1976**, *41*, 2855.

(11) Spencer, H. K.; Cava, M. P.; Garito, A. F. *Chem. Commum.* **1976**, 966.

(12) Pittman, C. U.; Narita, M.; Liang, Y. F. *Macromolecules* **1976**, *9*, 360.

(13) Ueno, Y.; Masuyama, Y.; Okawara, M. *Chem. Lett.* **1975**, 603.

(14) Saito, G. *Pure Appl. Chem.* **1987**, *59*, 999.

(15) Saito, G.; Enoki, T.; Toriumi, K.; Inokuchi, H. *Solid State Commun.* **1982**, *42*, 557.

(16) Jerome, D.; Mazaud, A.; Ribault, M.; Bechgaard, K. *J. Phys. Lett.* **1980**, *41*, 95.

(17) Saito, G.; Kumagai, H.; Katayama, C.; Tanaka, C.; Tanaka, J.; Wu, P.; Mori, T.; Imaeda, K.; Enoki, T.; Inokuchi, H.; Higuchi, Y.; Yasuoka, N. *Isr. J. Chem.* **1986**, *27*, 319.

0022-3263/94/1959-6519$04.50/0

Scheme 1. Synthesis of TTF Derivatives 1 and 2

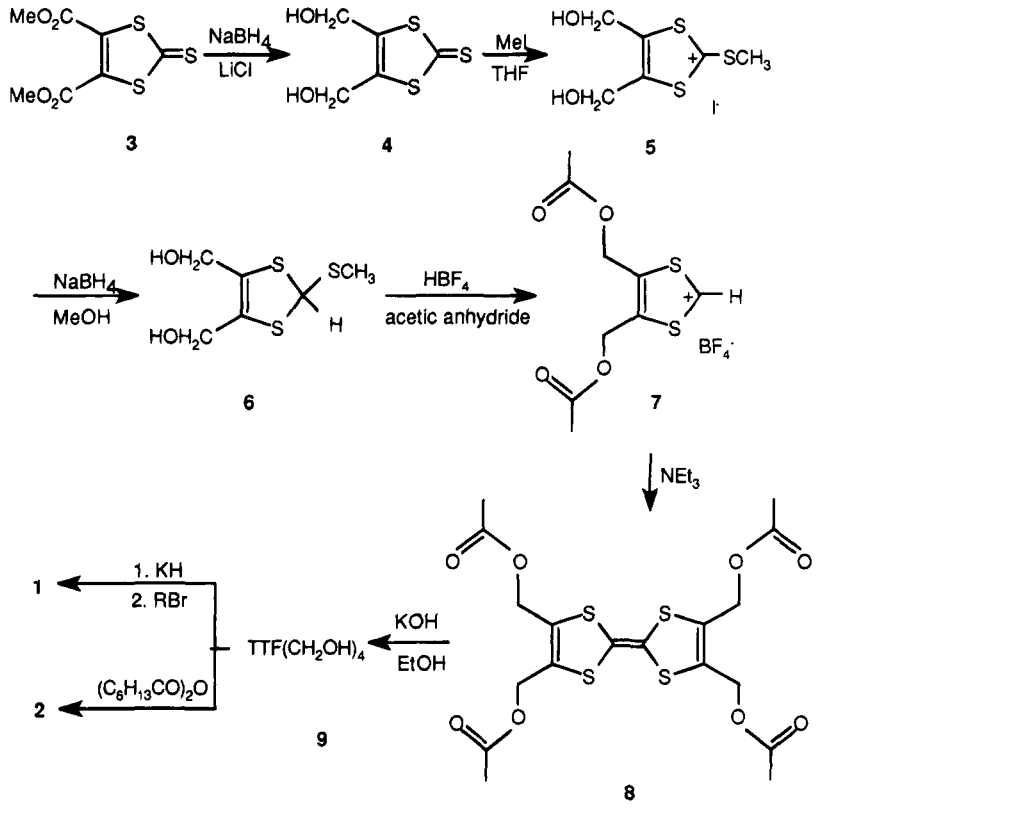

of one member of the family, **1** (n = 7), sandwiched symmetrically between two indium tin oxide electrodes (in a device similar to that described earlier for a liquid crystalline porphyrin sandwich cell[18,19]). The absorption spectrum and conductivity of the charge transfer complexes of **1** (n = 10) with iodine are also described.

Results and Discussion

Synthesis. The ether derivatives **1** are synthesized by the route shown in Scheme 1. Dimethyl 2-thiono-1,3-dithiole-4,5-dicarboxylate **3**, which is available from a one-step reaction from ethylene trithiocarbonate,[20] was chosen as starting material. By controlling the reaction temperature (ca. −10 °C) for a sodium borohydride reduction of **3**, it proved possible to suppress 1,4-reduction, producing the desired diol **4** in reasonable yield (70%).[21,22] Although the direct oxidation of 1,3-dithiole-2-thione with peracetic acid has been reported to give 1,3-dithiolium hydrogen sulfate, eq 1,[23] the same conditions failed to produce isolable quantities of the corresponding bis-hydroxymethylated salt, eq 2, the organic salt thus formed having been found to be unstable at temperatures above 10 °C. In contrast, the organic salt of 4,5-bis-(hydroxymethyl)-2-(methylthio)-1,3-dithiolium iodide (**5**), obtained by methylation of **4** with excess methyl iodide, is quite stable. By reducing **5** with sodium borohydride in methanol at 0 °C, 4,5-bis(hydroxymethyl)-2-(methylthio)-1,3-dithiole (**6**) was obtained in 90% yield. Protection of the hydroxy groups of **6** proved to be necessary before dethiomethylation (−SCH_3) could be accomplished: treatment of **6** with fluoroboric acid in acetic anhydride produced 4,5-bis(acetoxymethyl)-1,3-dithiolium fluoroborate (**7**), which was immediately treated with triethylamine in acetonitrile, producing 2,3,6,7-tetrakis(acetoxymethyl)tetrathiafulvalene (**8**) in 77% yield. Hydrolysis of **8** was accomplished by heating under reflux with potassium hydroxide in ethanol, giving 2,3,6,7-tetrakis(hydroxymethyl)tetrathiafulvalene (**9**) as a yellow-orange powder (92%). Alkylation of the anion (or multianion) of **9** by various long chain alkyl bromides was carried out in dimethyl sulfoxide (DMSO) at room temperature. In the presence of hexamethylphosphoric triamide (HMPA), the rate of alkylation was enhanced, leading to etherification at all four hydroxymethyl groups to produce 2,3,6,7-tetrakis(alkoxymethyl)tetrathiafulvalene **1**. Alternatively, esterification was achieved by treatment of **9** with alkanoic anhydride in the presence of catalytic amounts of 1-naphthalenesulfonic acid to give **2** in 73% yield.

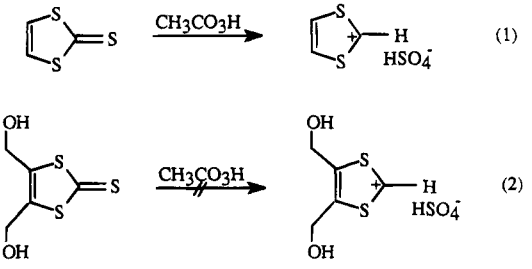

Charge Transfer Complexes (CTC). A CTC complex of **1** (n = 10) with iodine was prepared by mixing stoichiometric quantities of the two reagents in CH_2Cl_2. Unfortunately, attempts to grow a crystal of sufficient size and quality for X-ray analysis were not successful.

(18) Gregg, B. A.; Fox, M. A.; Bard, A. J. *J. Phys. Chem.* **1990**, *94*, 1586.
(19) Liu, C.-Y.; Pan, H. L.; Fox, M. A.; Bard, A. J. *Science* **1993**, *261*, 897.
(20) O'Connor, B. R.; Jones, F. N. *J. Org. Chem.* **1970**, *35*, 219.
(21) Brown, H. C. *Boranes in Organic Chemistry*; Cornell University Press: New York, 1972.
(22) Hajos, A. *Complex Hydrides and Related Reducing Agents in Organic Synthesis*; Elsevier Scientific: New York, 1979.
(23) Klingsberg, E. *J. Am. Chem Soc.* **1964**, *86*, 5290.

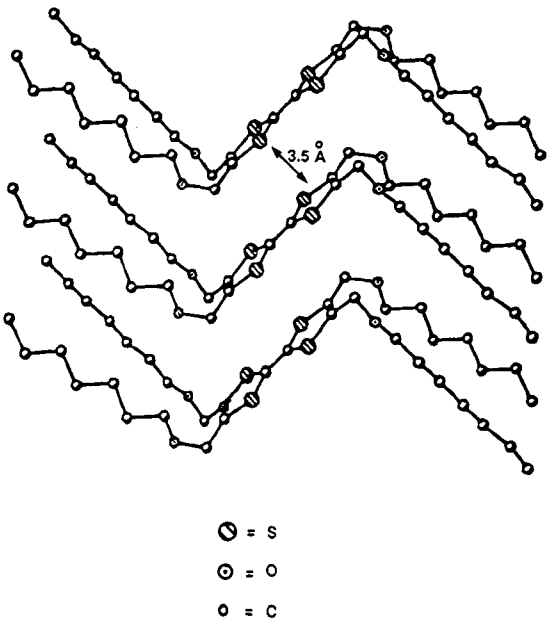

Figure 1. A crystal packing diagram for **1** (n = 7).

Although the formation of a CTC of **1** (n = 10) with TCNQ was also attempted, pure products could not be obtained because of the completely different solubility properties of **1** (favored in nonpolar solvents) and TCNQ (favored in polar solvents). However, the formation of both the iodine and TCNQ charge transfer complexes can be monitored by changes in their solution absorption spectra (see below).

Crystal Structure of 1 (n = 7). A crystal packing diagram for **1** (n = 7), obtained by X-ray analysis, is shown in Figure 1. The relevant bond lengths and angles and torsional angles are listed in supplementary material as Tables 1 and 2. This X-ray structure (**1** (n = 7)) shows a tightly packed bent structure about a flat central group. The two five-member rings of the tetrathiafulvalene core are located in the same plane, with a deviation of less than ±0.01 Å. The shortest intermolecular distance between the two tetrathiafulvalene moieties of **1** (n = 7) is 3.5 Å. Presumably, hydrophobic aggregation of the alkyl chains of **1** (n = 7) pushes the tetrathiafulvalene units close together in the crystal, with the resulting decreased stacking distance forcing the central group into a planar conformation. On one side of the tetrathiafulvalene core, the alkyl chains point upward and on the other side downward. Although the reason for the opposite dispositions of the alkyl chains is not clear, similar observations have been reported for TTF-$(SC_{10}H_{21})_4$.[14]

This structure differs substantially from the crystal structures obtained for both tetrakis(methylthio)-TTF[24] (**10**) and bis(ethylenedithio)-TTF[25] (**11**), in which there is a significantly longer separation between the two tetrathiafulvalene moieties (3.7–3.8 Å). In both **10** and **11**, the tetrathiafulvalene core is planar and the two five-member rings have a folded envelope-like structure: e.g., **10** has an angle of 19–24° along the C–S–C bonds in the heterocycle.[14]

Physical Properties. Neutral Molecules. Although the X-ray analysis provides evidence for strong

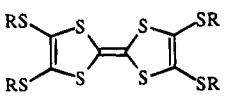

10

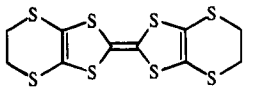

11

π,π-intermolecular interactions in **1** (n = 7), causing it to exist as a stacked solid, it melts cleanly and shows no evidence of an intermediate liquid crystalline phase. Nor did an examination of solid crystals of other members of family **1** or of **2**, either by differential scanning calorimetry (DSC) or under a polarizing microscope, give any evidence of a stable mesophase in any of the compounds.

The melting points of **1** are plotted against the length of the appended alkyl chains in Figure 2. No monotonic relationship between the alkyl chain length and the observed melting points can be found, but this plot does have a similar profile to that reported for TTF$(SC_nH_{2n+1})_4$, n = 1–18.[14,17] As with the thioether series, the lowest melting point is observed for **1** (n = 5).

Cyclic voltammetry shows the first and second oxidations of **1** (n = 3, 5, 7) and of **2** to be completely reversible one-electron transfers. The half-wave potentials for **1**, listed in Table 1, are very close to that of the parent TTF. Differences in the length of the alkyl chains for **1** have no effect on the electrochemical oxidation potential. Compound **2** is less easily oxidized than either the parent TTF or **1** (n = 3, 5, 7), presumably because of electron withdrawal by the ester group.

Charge Transfer Complexes (CTC). Elemental analysis of the CTC of **1** (n = 10) with iodine, prepared by titration, reveals a 1:1 ratio of the cation radical **1** (n = 10) to I_3^-. The electron spin resonance (ESR) of this solid shows a broad, unsplit ESR signal.

With quantitative absorption spectroscopy, it can be shown that the equilibrium constants for formation of CTCs between **1** (n = 6, 8, and 10) and TCNQ (K_{eq} = −2.7 ± 0.2) are similar to that reported for the CTC of TTF with TCNQ (K_{eq} = −2.4),[26] Table 2. Although these compounds have similar equilibrium constants, their solubilities vary greatly.

Absorption Spectra. Neutral Molecules. Figure 3 shows the absorption spectra of **1** (n = 7) as a solid thin film (solid line) and in solution (dashed line). The solution phase absorption spectra of **1** (n = 3, 5, and 7) are identical to those of TTF and are independent of the length of the alkyl chains, Table 3. In an exciton model for strong supramolecular interactions in the solid state, three terms contribute to the position of the spectral maximum:[27] $E°$ (the absorption maximum in solution), D (the energy change caused by multimer formation), and V (the energy of the exciton splitting), eq 3.[27]

$$\lambda_{max} = E° \pm D \pm V \qquad (3)$$

The solid phase spectrum shows no spectral shifts characteristic of long-range exciton interaction, despite the clear existence of strong intermolecular interactions enforced by π stacking, as implied by the X-ray data.

Charge Transfer Complexes. Figure 4 shows the absorption spectra of the 1:1 CTCs of **1** (n = 7) (solid line) and of TTF (dashed line) with iodine in CH_2Cl_2. The absorption spectra of the CTCs of **1** with iodine in CH_2Cl_2 are independent of alkyl chain length. The absorption

(24) Saito, N.; Saito, G.; Inokuchi, H. *Chem. Phys.* **1983**, *76*, 79.
(25) Saito, G.; Enoki, T.; Toriumi, K.; Inokuchi, H. *Solid State Commun.* **1982**, *42*, 557.
(26) Wheland, R. C. *J. Am. Chem. Soc.* **1976**, *98*, 3926.
(27) Fox, M. A.; Pan, H.-L.; Liu, C.-Y.; Bard, A. J. *J. Chin. Chem. Soc.* **1993**, *40*, 321.

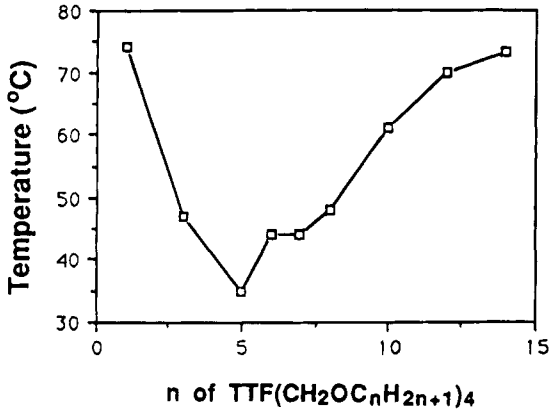

Figure 2. The effect of alkyl chain length on the melting points of **1**.

Table 1. Electrochemical Oxidation Potentials of 1 (n = 3, 5, 7) and 2[a]

	TTF	1 (n = 3)	1 (n = 5)	1 (n = 7)	1b
E_0^1	0.31	0.31	0.31	0.31	0.46
E_0^2	0.68	0.63	0.63	0.63	0.77

[a] Potentials (±0.01 V) are reported in V *vs* SCE and were measured at a concentration of ca. 10^{-4} M in 0.1 M tetrabutylammonium perchlorate in anhydrous CH_3CN as a degassed solution at room temperature oni a platinum flag electrode.

Table 2. Equilibrium Constants for Charge Transfer Complexation of TTF, 1 (n = 6, 8, 10), and 2 with TCNQ[a]

	TTF	1 (n = 6)	1 (n = 8)	1 (n = 10)	2
K_{eq}	−2.4 ± 0.2	−2.6 ± 0.2	−2.7 ± 0.2	−2.8 ± 0.2	−2.7 ± 0.2

[a] All measurements in anhydrous acetonitrile at room temperature.

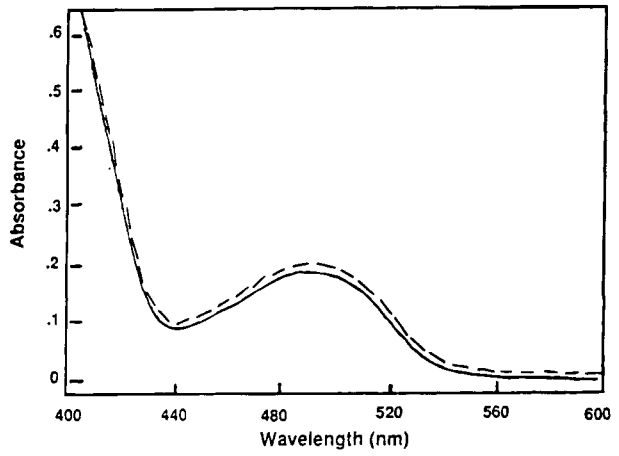

Figure 3. Absorption spectra of **1** (n = 7) in the solid state (solid line) and in CH_2Cl_2 solution (dashed line). Spectral intensities are in arbitrary units normalized to the absorption maximum.

maximum for the CTC of TTF (λ_{max} = 435, 580 nm)[28] is clearly blue-shifted from that of **1** (n = 7, λ_{max} = 455, 625 nm). This is unexpected, for the absorption spectra of **1** (n = 7) and TTF (as neutral molecules) are identical, as are their oxidation potentials.

In the solid phase, the absorption spectrum of the CTC of **1** (n = 7) with iodine is broadened and slightly red-shifted from that observed in solution, Figure 5. No

Table 3. Molar Extinction Coefficients of TTF and 1 (n = 3, 5, 7)[a]

	TTF	1 (n = 3)	1 (n = 5)	1 (n = 7)
λ_{max} (nm) ± 2	370, 490	370, 490	370, 490	370, 490
ϵ (cm^{-1} M^{-1}) ± 100	4000, 500	4100, 500	4100, 500	4000, 500

[a] All measurements were made in aerated CH_2Cl_2 at room temperature.

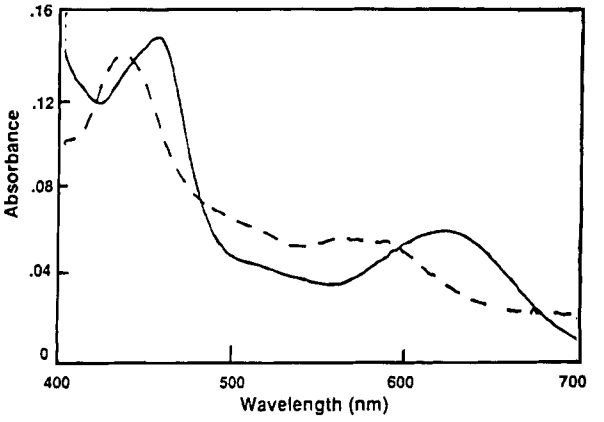

Figure 4. Absorption spectra of a 1:1 charge-transfer complexes with iodine in methylene chloride of **1** (n = 7) (solid line) and TTF (dashed line).

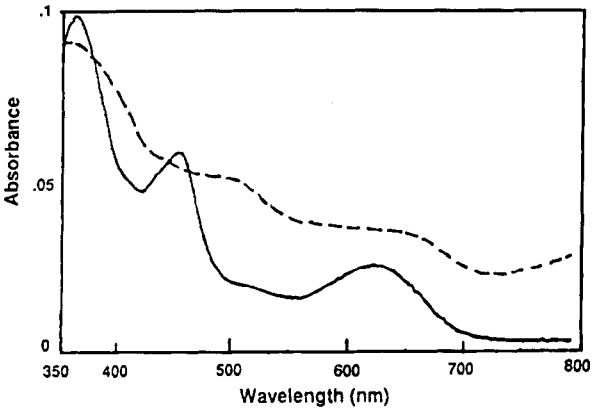

Figure 5. Absorption spectra of a 1:1 charge-transfer complex of **1** (n = 7) with iodine in methylene chloride solution (solid line) and in the solid state (dashed line).

obvious absorption beyond 700 nm is observed in dilute solution (solid line), but an absorption near 800 nm is evident in the solid phase (dashed line). This suggests that the CTC of **1** (n = 7) in the solid state can undergo enhanced excitonic coupling and that the CTC of **1** (n = 7) is more ordered in the solid state than as a neutral crystal.

Dark Conductivity. Neutral Molecules. The dark conductivity of a thin layer **1** (n = 7), as measured by a two-probe method,[29] is high (10^{-6}–10^{-7} Ω^{-1} cm^{-1}). From eq 4, an Arrhenius plot of the temperature dependence of observed dark conductivity (σ_d) yields an activation energy ΔE for **1** (n = 7) of ca. 0.74 eV with a fitting parameter, σ_o, of 1.05 $\Omega^{-1}cm^{-1}$.

$$\sigma_d = \sigma_o \exp[-\Delta E/(2kT)] \quad (4)$$

where k is Boltzmann's constant, T is the absolute temperature, and σ_o is a preexponential term.

(28) Wudl, F.; Smith, G. M.; Hufnagel, E. J. *Chem. Commun.* **1970**, 1453.

(29) Meier, H.; Albrecht, W.; Kisch, H.; Nüsslein, F. *J. Phys. Chem.* **1989**, *93*, 7726.

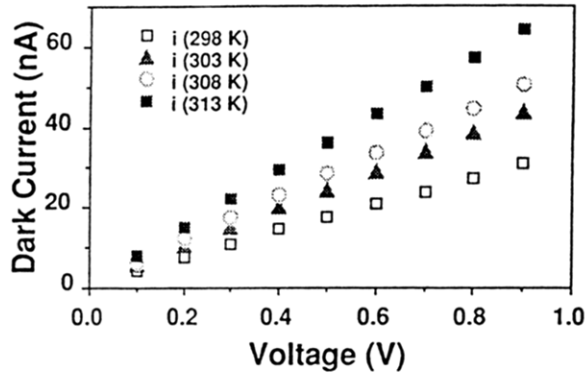

Figure 6. Dependence of temperature-dependent dark current on applied voltage across a thin (3 μm) film of **1** ($n = 7$).

In contrast, as a neutral molecule, TTF has a low dark conductivity (10^{-11}–10^{-12} Ω^{-1} cm^{-1}). The observed differences in the dark conductivities of these two compounds might derive from differences in their molecular structures: whereas **1** ($n = 7$) has a flat central core, TTF has an envelope structure.[25] Furthermore, the stacking distance is shorter in **1** ($n = 7$) than in TTF, thus allowing for greater intermolecular electronic delocalization through π,π contact.

When an external potential is applied across opposite faces of a 3 μm thick film of **1** ($n = 7$) sandwiched between optically transparent, conductive indium tin oxide plates, a linear relationship is observed in the dark between the observed current and the applied voltage: that is, the dark current I_d increases with field strength up to +1.0 V in the range of our study, Figure 6. This is typical ohmic behavior. At higher temperatures, a larger slope is observed. No such temperature-dependent conductivity in solid TTF (neutral molecules) has been reported,[25] and most organic crystals have low dark conductivities (10^{-9}–10^{-13} Ω^{-1} cm^{-1}), which are assumed to be temperature-independent.[29] The unusual temperature dependence observed with **1** ($n = 7$) may therefore reflect a higher level of population of trap sites in this derivative and/or greater nonrigidity within the unit cell, permitting thermally-assisted motions to enhance electronic coupling.

Charge Transfer Complexes. The CTC of TTF with iodine is known to have high conductivity.[2-5] Similarly, **1** ($n = 10$) doped with iodine (1:1) shows metallic behavior as a thin film with a dopant concentration-dependent conductivity ranging up to 10^3 Ω^{-1} cm^{-1}. No dark chemical degradation of this CTC could be observed over a period of 8 months, when monitored by conductivity measurements, absorption spectroscopy, or elemental analysis.

Photocurrent Induced by Irradiation of 1 ($n = 7$) in a Sandwich Photocell. Neutral Molecules. The same 3 μm thick ITO–**1** ($n = 7$)–ITO (indium tin oxide) sandwich cell described above, when irradiated at 490 nm (ca. 10^{15} photons/cm^2), shows a photoconductive response that depends on illumination intensity, the film's absorption extinction coefficient, and cell thickness. This response is parallel to what had been observed earlier in a ITO-liquid crystalline porphyrin-ITO sandwich cell,[18,19,27] although the magnitude of the short-circuit photocurrent and open-circuit photovoltage are substantially lower than in porphyrin-based cells. The short-circuit photocurrent quantum yield, Figure 7a, observed in a manually light-chopped ITO–**1** ($n = 7$)–ITO cell is ca. 10^{-6}.

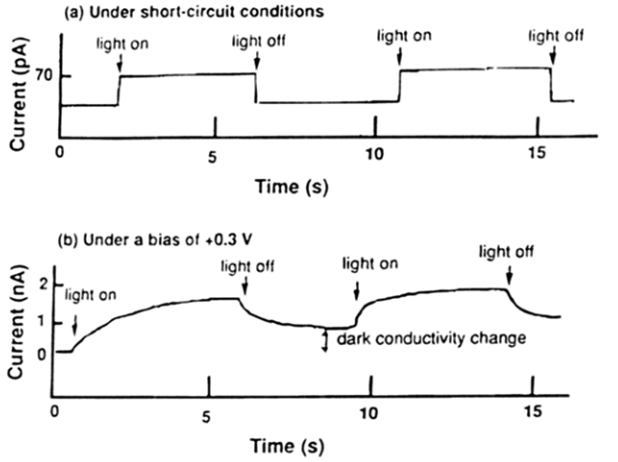

Figure 7. Photoeffects in a 3 μm thick ITO–**1** ($n = 7$)–ITO sandwich cell upon irradiation at 490 nm (ca. 10^{15} photons/cm^2) with a manual light chop. (a) Short-circuit photocurrent; (b) polarization current under a bias of +3.0 V.

Several phenomena can explain the low photocurrent. First, exciton formation may occur only inefficiently, as is reflected in the absorption extinction coefficient at the excitation wavelength of the experiment. The low extinction coefficient also increases the depth of light penetration, making the interface distribution of excited states more diffuse. Second, different crystal packings give different photoconductivities, as has been demonstrated with phthalocyanines as photoreceptors.[30] Third, high bulk dark conductivity of **1** ($n = 7$) may enhance charge mobility through the solid layer, producing efficient exciton quenching. Finally, charge injection at the ITO interface may be significantly slower than with other π-stacked arrays.

Charge Transfer Complexes. Irradiation of the 1:1 CTC of **1** ($n = 10$) with iodine with visible or long wavelength ultraviolet light produces no measurable photocurrent in an analogous sandwich cell. Since the conduction band of ITO lies at about ~−0.8 V vs NHE[31] and $\mathbf{1}^+/\mathbf{1}^{2+}$ for **1** ($n = 10$) is at +0.9 V vs NHE, a photon with a wavelength of 730 nm (~1.7 eV) or shorter is sufficiently energetic to achieve exothermic charge injection into ITO. The presence of a lower energy electronic transition in the absorption spectrum of the **1** ($n = 10$)·I_3^- CTC, however, provides a lower energy relaxation pathway that would be incompatible with efficient photosensitized electron injection.[32] Similarly, from the calculated bandwiths of the analogous CTC of TTF with I_2, a low energy transition at ~0.9 eV has been reported,[33] and as a result, no charge injection has been observed in this system. Therefore, charge transfer complexes of TTF and its derivatives are not suitable components for photosensitization of ITO sandwich short-circuit photovoltaic devices.

Photocurrent under an External Bias. Neutral Molecules. A slow increase in attainable photocurrent in an ITO–porphyrin–ITO photocell is observed upon applying an external field during irradiation. Such a

(30) Sharp, J. H.; Lardon, M. *J. Phys. Chem.* **1968**, *72*, 3230.
(31) Bard, A. J. *Encyclopedia of Electrochemistry of the Elements*; Marcel Dekker: New York, 1973 and references therein.
(32) Gerischer, H.; Willig, F. *Top. Curr. Chem.* **1976**, *61*, 33.
(33) Cowan, D. O.; Mays, M. D.; Kistenmacher, T. J.; Poehler, T. O.; Beno, M. A.; Kini, A. M.; Kowk Y.-K.; Carlson, D.; Xiao, L.; Novoa, J. J.; Whangbo, M.-H. *Mol. Cryst. Liq. Cryst.* **1990**, *181*, 43 and references therein.

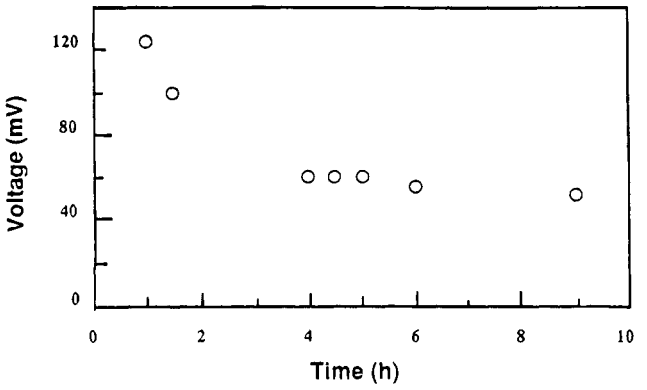

Figure 8. Duration of trapped charge in an ITO−**1** (n = 7)−ITO sandwich photocell prepolarized under a +1.0 V bias and irradiated with a 5 W tungsten lamp for 5 s.

slow increase in photocurrent has been defined as a photopolarization current.[33] Shown in Figure 7b is the photopolarization current (against a baseline current measured in the dark) obtained in an ITO−**1** (n = 7)−ITO sandwich photocell under +0.3 V bias under the otherwise identical conditions to that employed for the short-circuit measurement, Figure 7a. The fast-response short-circuit photocurrent, corresponding to immediate excitonic charge injection at the irradiated ITO−sensitizer interface, is small under these conditions and cannot be seen on the current scale in Figure 7b. The slow increase in polarization current is caused by sequential electron hopping (from one trap site to another) of charges separated by the external electric field. The buildup of charge carriers apparently affects dark conductivity: even when the light was off, a slow change in the baseline dark current can be seen under the applied bias. That is, the baseline level of dark conductivity cannot be quickly restored at short times after polarization. This indicates that some charge carriers survive for at least a short time period after the termination of irradiation.

The relaxation of this charge separation is shown in Figure 8. There are two modes for charge recombination: a slow process in the dark, Figure 8, and an instantaneous relaxation in the light, Figure 9. These measurements are carried out under short-circuit conditions but with a high impedance (>10^{12} Ω) in the dark after the thin film of **1** (n = 7) had been polarized under irradiation. This result is consistent with our expectations that **1** (n = 7), like CdS[34] and the porphyrins described earlier, can produce trapped charge carriers in the bulk. However, although charge is trapped in **1** (n = 7), most of the stored voltage is lost after 2 h. This is far too short a storage period for practical applications and is several orders of magnitude lower than has been observed in the solid state pophyrin thin film cells described elsewhere.[19] This short charge trapping duration is probably attributable to the much lower dark resistance of **1** (n = 7) than of the other light absorbers. That charge remains separated at all, despite efficient electronic coupling in the dark, reflects an unusual stability of the cation radical of **1** (n = 7).

Figure 9 compares the wavelength response for the release of trapped charge from the photopolarized cell with the absorption spectrum of **1** (n = 7). This parallel suggests that the excited states of **1** (n = 7) take part in the release of the trapped charge.

(34) Kallmann, H.; Rosenberg, B. *Phys. Rev.* **1955**, *97*, 1596.

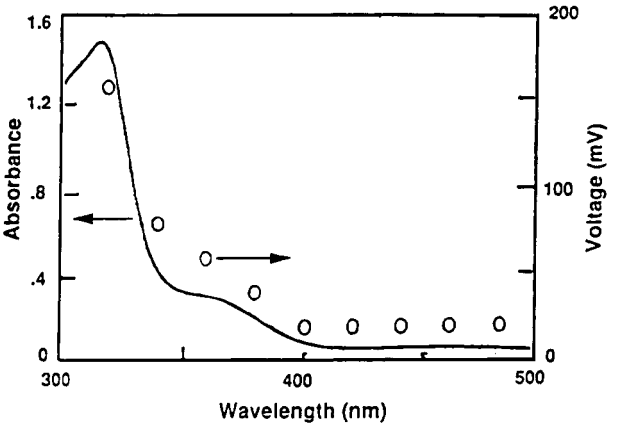

Figure 9. Wavelength response for photodischarge of an ITO−**1** (n = 7)−ITO sandwich photocell (open circles) charged as described in Figure 8 and superimposed on a solid state absorption spectrum of **1** (n = 7).

Conclusions

Although the new family of tetrakis(alkoxymethyl)-substituted TTF derivatives **1** shows no evidence of a liquid crystalline mesophase, these compounds stack in the solid state to induce sufficient long-range order to permit formulation of thin films that are useful as components of optoelectronic devices. Many of this family's physical properties closely resemble those of the parent tetrathiafulvalene, although anomalously high dark conductivity is observed for **1** (n = 7). As with tetrathiafulvalenes, these compounds can form highly conductive charge transfer complexes.

Experimental Section

Materials. Dimethyl acetylenedicarboxylate, alkyl bromides, and ethylene trithiocarbonate (Aldrich) were used as received. Tetrahydrofuran (THF) was distilled from sodium and benzophenone immediately before use. Toluene, triethylamine, acetonitrile, and DMSO were distilled from 4 Å molecule sieves before use. HMPA was distilled from barium oxide and was stored under nitrogen. Solvents for spectroscopic studies were spectral grade and were used as received. Chromatography was conducted via a Si-60 (230−400 mesh) flash column chromatography. Tetracyanoquinodimethane (TCNQ, Aldrich) was sublimed twice before use.

X-ray Analysis. The analyzed crystal was a thin plate of approximate dimensions: 0.04 × 0.35 × 0.84 mm. The data were collected at room temperature on a Nicolet P3 diffractometer using a graphite monochromator with Mo Kα radiation (λ = 0.7107 Å). The crystal system is monoclinic and the space group is $C2/c$. The lattice parameters were obtained by the least-squares refinement of 40 reflections with 12.1 < 2θ < 20.7°; a = 40.40(3), b = 5.328(3), c = 19.70(2) Å, β = 106.06(6)°, V = 4075(6) Å^3, r_{calc} = 1.17 g cm^{-3} (298 K) for Z = 4 and F(000) = 1568. The data were collected from 4.0 to 45.0° in 2θ using the ω scan technique, with a 1.2° scan range in ω at 3−6° min^{-1}. A total of 5444 reflections were measured, of which 2682 were unique (R for averaging equivalent reflections = 0.042), where h ranged from 0 → 41, k ranged from −6 → 6 and l ranged from −19 → 19. Four reflections (5,1,1; −7,1,4; −6,0,−2; 7,1,−4) were remeasured every 96 reflections to monitor instrument and crystal stability. A smoothed curve of the intensities of

these check reflections was used to scale the data. The scaling factor ranged from 0.875–1.01 with the intensities of the standards showing a smooth, gradual decrease in intensity throughout the course of the data set. The data were corrected for Lp effects and absorption. The absorption correction was based on crystal face measurements. The transmission factors ranged from 0.9055–0.9884 for $\mu = 2.572$ cm^{-1}. Data reduction and decay correction were performed using the SHELXTL-Plus software package.[35] The structure was solved by direct methods and refined by full-matrix least-squares fit with anisotropic thermal parameters for the non-H atoms. The hydrogen atoms were calculated in idealized positions (C–H 0.96 Å) with a refined isotropic thermal parameter. The molecule lies on an inversion center at 1/4, 1/4, 0. Reflections having $F_o < 6(\sigma(F_o))$ were considered unobserved (1104 reflections). The function, $\sum w(|F_o| - |F_c|)^2$, was minimized, where $w = 1/(\sigma(F_o))^2$ and $\sigma(F_o) = \{.5kI^{-1/2}[(\sigma(I))^2 + (0.02I)^2]^{1/2}\}$. The intensity, I, is given by $(I_{peak} - I_{background}) \times$ (scan rate); where 0.02 is a factor to downweight intense reflections and to account for instrument instability and k is the correction due to Lp effects, absorption and decay. $\sigma(I)$ was estimated from counting statistics; $\sigma(I) = [(I_{peak} + I_{background})^{1/2} \times$ (scan rate)]. A total of 242 independent parameters were refined to a final $R = 0.0593$ using 1578 reflections, with a $wR = 0.0683$ and a goodness of fit = 1.817. The R for all data was equal to 0.105, with a $wR = 0.0814$. The maximum $|\Delta/\sigma| < 0.1$ in the final refinement cycle and the minimum and maximum peaks in the final difference electron density map were −0.27, 0.61 e$^-$/Å,[36] respectively. Neutral atom scattering factors for the non-H atoms were taken from Cromer and Mann,[37] with the anomalous-dispersion corrections taken from the work of Cromer and Liberman.[36] The scattering factors for the H atoms were obtained from Stewart, Davidson, and Simpson.[38] Values used to calculate the linear absorption coefficient are from the *International Tables for X-ray Crystallography* (1974).[39] All figures were generated using SHELXTL-PLUS.[34]

Cell and Films. The preparation of solid state photocells used for the polarization measurements and that of the thin films used in the optical measurements have been previously described.[16]

Instrumentation. Melting points were determined with a Mel-Temp device and are uncorrected. Phase transitions were characterized by differential scanning calorimetry (DSC) with either a Perkin-Elmer TG-7 or Mettler FP 80/84 instrument. ^{1}H and ^{13}C nuclear magnetic resonance spectra were recorded at 300 MHz or 75 MHz, respectively, on a QE-300 spectrometer. Cyclic voltammetry was performed with PAR a Model 173 potentiostat and a Model 175 universal programmer, coupled with a Model 179 digital coulometer. The signal was recorded on a Houston Instruments 2000 x-y recorder. The working electrode was Pt and the reference electrode was Ag/AgNO$_3$; the scan rate was 100 mV/s. Absorption spectra were measured on a Hewlett Packard 8451A single beam spectrophotometer using unpolarized light. ESR spectra were recorded by a Brucker ER 300 spectrometer with sweep time 21 s; sweep width 200 G; and frequency 9.8 GHz. The conductivity is measured by the techniques of four probe or two electrode contacts.[29] Temperature control is carried out with a thermal processor (Mettler) coupled with a FP82 hot stage.

Synthesis. 4,5-Bis(hydroxymethyl)-2-thiono-1,3-dithiole (4). A solution of dimethyl 2-thiono-1,3-dithiole-4,5-dicarboxylate (**3**)[9] (980 mg, 3.9 mmol) in THF (10 mL) was added dropwise to a solution of $NaBH_4$ (1 g, 26.4 mmol) and LiCl (100 mg, 2.3 mmol) in 10 mL of MeOH and 5 mL of THF. The solution was maintained at ca. −10 °C by external cooling while the diester was added. A substantial evolution of gas accompanied the addition. The reaction mixture was stirred vigorously at 0–10 °C for 3 h after the addition was complete; chilled water (60 mL, 5 °C) was then added. The resulting mixture was extracted with chilled ethyl acetate (−10 °C, 50 mL, 3×). The combined organic extract was washed with brine (50 mL, 2×), dried over $MgSO_4$, and concentrated. The yellow crude product was recrystallized from dry acetone and hexane to give **4** (70%): mp 86–87 °C, light yellow needles. ^{1}H NMR ($CDCl_3$): δ 4.6 (d, $J = 6$ Hz, 4 H), 4.9 (t, $J = 6$ Hz, 2 H). ^{13}C NMR ($CDCl_3$): δ 57.9, 143.0, 213.8. MS (CI), m/e: calcd for $C_5H_6O_2S_3$ 194.960820, found 194.958826.

4,5-Bis(hydroxymethyl)-2-(methylthio)-1,3-dithiolium Iodide (5). Diol **4** (5.4 g, 27.7 mmol) was dissolved in 30 mL of dry THF and excess methyl iodide (ca. 20 mL) was carefully added. This mixture was stirred and heated under reflux for 6 h under nitrogen. The precipitate was filtered to give 9.1 g of **5** (98%): mp 114 °C dec, yellow powder. ^{1}H NMR (D_2O): δ 3.0 (s, 3H), 4.5 (s, 2H), 4.7 (s, 4H). ^{13}C NMR (D_2O): δ 24.4, 58.6, 152.2, 204.8. MS (FAB), m/e: calcd for $C_6H_9O_2S_3^+$ 208.976470, found 208.978273.

4,5-Bis(hydroxymethyl)-2-(methylthio)-1,3-dithiole (6). Into a 250 mL round-bottom flask containing a magnetic stirrer were placed **5** (9.1 g, 27 mmol) and 100 mL of methanol (absolute). The mixture was stirred and cooled in an ice bath with sodium chloride. The temperature was regulated to ca. 0–5 °C while sodium borohydride (1.3 g, 35 mmol) was added cautiously. After the addition was complete, stirring was continued for 1 h. Elevating temperature over 40 °C during workup should be avoided or **6** will decompose very quickly. The colorless methanol solution was concentrated and chilled to induce crystallization of **6**; any color change indicated decomposition of **6**. Ice–water (50 mL) was then added and the resulting solution was extracted with ethyl acetate (3 × 200 mL). The combined ethyl acetate solution was then washed with brine (3 × 30 mL), dried over magnesium sulfate, filtered, and concentrated on a rotary evaporator to give, after crystallization from chilled methanol, 5.0 g of **6** (90%): mp 62 °C dec, white crystals. ^{1}H NMR ($CDCl_3$): δ 3.1 (s, 3H), 4.3 (m, 6H), 6.0 (s, 1H). ^{13}C NMR ($CDCl_3$): δ 11.2, 56.6, 57.3, 129.0. MS (FAB), m/e: calcd for $C_5H_6O_2S_3$, 209.977551, found 209.975073.

2,3,6,7-Tetrakis(acetoxymethyl)tetrathiafulvalene (8). A solution of **6** in acetic anhydride (40 mL) was cooled to ca. −10–0 °C while a fluoroboric acid solution (48%) was added dropwise. When the addition was complete, stirring was continued for 30 min, and anhydrous ether was added (250 mL). The resulting solution was then chilled in a freezer overnight. The ether layer was then decanted and the nearly white precipitate was washed with 50 mL of ether and dried

(35) Sheldrick, G. M. (1989). SHELXTL-*PLUS* (Version 4.1). Siemens Analytical X-ray Instruments, Inc., Madison, WI.
(36) Cromer, D. T.; Liberman, D. *J. Chem. Phys.* **1970**, *53*, 1891.
(37) Cromer, D. T.; Mann, J. B. *Acta Crystallogr.* **1968**, *A24*, 321.
(38) Stewart, R. F.; Davidson, E. R.; Simpson, W. T. *Phys. Chem.* **1965**, *42*, 3175.
(39) *International Tables for X-ray Crystallography*; Kynoch Press: Birmingham, 1974; p 55.

under vacuum to give 4,5-bis(acetoxymethyl)-1,3-dithiolium fluoroborate (**7**). Compound **7**, which was used directly, was dissolved in 40 mL of acetonitrile in a 250 mL round-bottom flask. The solution was stirred at room temperature; 20 mL of triethylamine was then slowly added until the formation of yellow crystals was obvious. Another 5 mL of amine was then added. The resulting solution was stirred for an additional 20 min before water (150 mL) was slowly added to precipitate the product. The precipitate was filtered, washed with water, and dried under vacuum. The crude product was then dissolved in ether, passed through a short basic aluminum oxide column, and recrystallized from hexane and dichloromethane to give **8** (77%): mp 131 °C, orange needles. ^{1}H NMR ($CDCl_3$): δ 2.1 (s, 12H), 4.9 (s, 8H). ^{13}C NMR ($CDCl_3$): δ 20.6, 57.9, 108.6, 129.6, 170.3. MS (CI), *m/e*: calcd for $C_{18}H_{20}O_8S_4$ 492.004105, found 492.004351.

2,3,6,7-Tetrakis(hydroxymethyl)tetrathiafulvalene 9. A mixture of tetraester **8** (2.0 g, 4 mmol) and KOH (1.6 g, 28 mmol) in 32 mL of a mixture of solvents (20 mL of MeOH, 10 of mL THF, and 2 mL of water) was heated at reflux overnight. THF (10 mL) was added after the solution had cooled to room temperature. The precipitate was filtered, washed with warm water (10 mL) and ethyl alcohol (10 mL), and dried under vacuum to give **9** (92%): mp 190 °C dec, yellow-orange powder. ^{1}H NMR (DMSO-d_6): δ 4.2 (s, 8H), 4.6 (s, 4H). ^{13}C NMR (DMSO-d_6): δ 57.1, 107.0, 132.1. MS (CI^+), *m/e*: calcd for $C_{10}H_{12}O_4S_4$ 323.961846, found 323.963193. IR (KBr) ν_{max} 3250, 2963, 2932, 2874, 1609, 1462, 1362, 1183, 961 cm^{-1}.

2,3,6,7-Tetrakis(alkoxymethyl)tetrathiafulvalene 1. General Method. Dry DMSO (2.0 mL) was slowly added to 110 mg of KH (27 mmol) under nitrogen. The solution was stirred for 10 min and HMPA (1.0 mL) was added. A solution of **9** (4.5 mmol) in 1.0 mL of DMSO was then slowly added. The resulting solution was stirred overnight and 27 mmol of 1-bromoalkane was then slowly added. After alkyl bromide was added, 20 mL of ether was added and the solution was extracted with water (2 × 10 mL) and brine (2 × 5 mL). The ether layer was then dried over magnesium sulfate, concentrated, and added to methanol (30 mL). This solution was then cooled in a freezer overnight to induce crystallization. Orange crystals (60–80%) were collected.

2,3,6,7-Tetrakis(1-methoxymethyl)tetrathiafulvalene 1 (*n* = 1) (62%): mp 74 °C. ^{1}H NMR ($CDCl_3$): δ 3.3 (s, 12H), 4.2 (s, 8H). ^{13}C NMR ($CDCl_3$): δ 58.1, 66.8, 108.2, 130.5. MS (FAB), *m/e*: calcd for $C_{10}H_{20}O_4S_4$ 380.024447, found 380.024562.

2,3,6,7-Tetrakis(1-propoxymethyl)tetrathiafulvalene 1 (*n* = 3) (73%): mp 47 °C. ^{1}H NMR ($CDCl_3$) δ 0.9 (t, J = 7 Hz, 12H), 1.6 (m, 8H), 3.4 (t, 8H), 4.2 (s, 8H). ^{13}C NMR ($CDCl_3$): δ 10.5, 22.8, 65.3, 72.1, 108.2, 130.7. MS (FAB), *m/e*: calcd for $C_{22}H_{36}O_4S_4$ 492.149647, found 492.152309.

2,3,6,7-Tetrakis(1-pentoxymethyl)tetrathiafulvalene 1 (*n* = 5) (68%): mp 35 °C. ^{1}H NMR ($CDCl_3$): δ 0.9 (t, J = 7 Hz, 12H), 1.3 (m, 16H), 1.6 (m, 8H), 3.4 (t, J = 7 Hz, 8H), 4.2 (s, 8H). ^{13}C NMR ($CDCl_3$): δ 13.9, 22.4, 28.1, 29.2, 65.2, 70.5, 108.3, 130.6. MS (FAB), *m/e*: calcd for $C_{30}H_{52}O_4S_4$ 604.271476, found 604.272731.

2,3,6,7-Tetrakis(1-hexoxymethyl)tetrathiafulvalene 1 (*n* = 6) (70%): mp 44 °C. ^{1}H NMR ($CDCl_3$): δ 0.9 (t, J = 7 Hz, 12H), 1.3 (m, 24H), 1.6 (m, 8H), 3.4 (t, J = 7 Hz, 8H), 4.2 (s, 8H). ^{13}C NMR ($CDCl_3$): δ 14.0, 22.5, 25.7, 29.5, 31.6, 65.2, 70.5, 108.2, 130.7. MS (FAB), *m/e*: calcd for $C_{34}H_{60}O_4S_4$ 660.334076, found 660.333399.

2,3,6,7-Tetrakis(1-heptoxymethyl)tetrathiafulvalene 1 (*n* = 7) (77%): mp 44 °C. ^{1}H NMR ($CDCl_3$): δ 0.9 (t, J = 7 Hz, 12H), 1.3 (m, 32H), 1.6 (m, 8H), 3.4 (t, J = 7 Hz, 8H), 4.22 (s, 8H). ^{13}C NMR ($CDCl_3$): δ 14.0, 22.6, 26.0, 29.1, 29.6, 31.8, 65.3, 70.6, 108.2, 130.7. MS (FAB), *m/e*: calcd for $C_{38}H_{68}O_4S_4$ 716.400048, found 716.398457.

2,3,6,7-Tetrakis(1-octoxymethyl)tetrathiafulvalene 1 (*n* = 8) (73%): mp 48 °C. ^{1}H NMR ($CDCl_3$): δ 0.9 (t, J = 7 Hz, 12H), 1.3 (m, 40H), 1.6 (m, 8H), 3.4 (t, J = 7 Hz, 8H), 4.22 (s, 8H). ^{13}C NMR ($CDCl_3$): δ 14.0, 22.6, 26.0, 29.2, 29.3, 29.5, 31.8, 65.2, 70.5, 108.1, 130.6. MS (FAB), *m/e*: calcd for $C_{42}H_{76}O_4S_4$ 773.470474, found 773.468563.

2,3,6,7-Tetrakis(1-decoxymethyl)tetrathiafulvalene 1 (*n* = 10) (75%): mp 61 °C. ^{1}H NMR ($CDCl_3$): δ 0.9 (t, J = 7 Hz, 12H), 1.3 (m, 56H), 1.6 (m, 8H), 3.4 (t, J = 7 Hz, 8H), 4.2 (s, 8H). ^{13}C NMR ($CDCl_3$): δ 14.1, 22.6, 26.0, 29.3, 29.4, 29.5, 29.5, 29.5, 31.9, 65.2, 70.5, 108.1, 130.7. MS (FAB), *m/e*: calcd for $C_{50}H_{92}O_4S_4$ 885.591204, found 885.573784.

2,3,6,7-Tetrakis(1-dodecoxymethyl)tetrathiafulvalene 1 (*n* = 12) (74%): mp 70 °C. ^{1}H NMR ($CDCl_3$): δ 0.9 (t, J = 7 Hz, 12H), 1.3 (m, 72H), 1.6 (m, 8H), 3.4 (t, J = 7 Hz, 8H), 4.2 (s, 8H). ^{13}C NMR ($CDCl_3$): δ 14.1, 22.6, 26.1, 26.1, 29.3, 29.5, 29.6, 29.6, 29.6, 29.6, 31.9, 65.3, 70.6, 108.2, 130.7. MS (FAB), *m/e*: calcd for $C_{58}H_{108}O_4S_4$ 996.713050, found 996.714122.

2,3,6,7-Tetrakis(1-tetradecoxymethyl)tetrathiafulvalene 1 (*n* = 14) (65%): mp 73 °C. ^{1}H NMR ($CDCl_3$): δ 0.9 (t, J = 7 Hz, 12H), 1.3 (m, 88H), 1.6 (m, 8H), 3.4 (t, J = 7 Hz, 8H), 4.2 (s, 8H). ^{13}C NMR ($CDCl_3$): δ 14.1, 22.6, 26.0, 29.3, 29.4, 29.6, 29.6, 29.6, 29.6, 29.6, 29.6, 31.9, 65.2, 70.6, 108.1, 130.6. MS (FAB), *m/e*: calcd for $C_{66}H_{124}O_4S_4$ 1108.838251, found 1108.838862.

2,3,6,7-Tetrakis(heptanoylmethoxyl)tetrathiafulvalene (2). A mixture of 100 mg of **9** (0.3 mmol), 300 mg of heptanoic anhydride (1.2 mmol), and 2 mg of 1-naphthalenesulfonic acid in DMSO (15 mL) was stirred overnight. Ether (20 mL) was then added. The ether solution was extracted with water (3 × 10 mL) and dried over magnesium sulfate. Methanol was added to induce crystallization of **2** (73%): mp 69 °C. ^{1}H NMR ($CDCl_3$): δ 0.9 (t, J = 7 Hz, 12H), 1.3 (m, 24H), 1.6 (m, 8H), 2.3 (t, J = 7 Hz, 8H), 4.9 (s, 8H). ^{13}C NMR ($CDCl_3$): δ 14.0, 22.4, 24.7, 28.7, 31.3, 33.9, 57.8, 108.4, 129.6, 173.1. MS (FAB), *m/e*: calcd for $C_{38}H_{60}O_8S_4$ 772.316236, found 772.314275.

CTC of 1 (*n* = 10) with Iodine. One equivalent of iodine (50 mg, 0.2 mmol) was added dropwise to a stirring solution of **1** (n = 10) (177 mg, 0.2 mmol) in dichloromethane (50 mL) at a rate of 5 mL/min in the dark.[5] A slow addition of iodine solution (ca. 5 mL/min) is required in order to obtain a high yield (60%). A substantial color change accompanied the addition. After being stirred for 10 min in the dark when the addition was completed, this solution was concentrated to ca. 40 mL. Methanol (40 mL) was added to induce crystallization. The resultant precipitate was recrystallized from dichloromethane/methanol, forming dark brown crystals.[40] CTC of **1** ($n \leq 8$) do not precipitate from methanol (or acetonitrile). This solution was kept in the dark for 2 days before crystals

(40) Bender, K.; Hennig, I.; Schweitzer, D.; Dietz, K.; Endres, H.; Keller, H. J. *Mol. Cryst. Liq. Cryst.* **1984**, *108*, 359.

were collected (60%). The resulting salt was then recrystallized twice from dichloromethane and methanol. UV (CH_2Cl_2) λ_{max} (ϵ): 455 (23 000), 625 (7000) nm. IR (KBr) ν_{max} 2922, 2853, 1115. Anal. Calcd for $C_{50}H_{92}O_4S_4I_3$: I, 30%; S, 10%. Found: I, 26%; S, 10%.

Attempted Synthesis of CTC of 1 (n = 10) with TCNQ. A solution of TCNQ (41 mg, 0.2 mmol) in acetonitrile (100 mL) was slowly added to a solution of **1** (n = 10) (177 mg, 0.2 mmol) in dichloromethane (50 mL) in the dark. This mixture was heated to reflux under nitrogen for 2 h and cooled to room temperature. The solvent of this mixture was allowed to evaporate slowly. Precipitation occurred over a period varying from several hours to three weeks. In nonpolar solvent (CH_2Cl_2) or benzene, neutral TCNQ contaminates the CTC; on the other hand, in polar solvents such as acetonitrile or methanol neutral **1** contaminates the CTC. The formation of CTC was characterized by monitoring its absorption in solution.[1,26] Since this CTC in the solid state was contaminated by either **1** (n = 10) or neutral TCNQ, no pure CTC solid crystal was obtained.

Acknowledgment. This work was supported by the U. S. Department of Energy, Office of Basic Energy Sciences, Fundamental Interactions Branch, and by the Robert A. Welch Foundation. We thank Dr. Vincent Lynch for help with the X-ray analysis and gratefully acknowledge very useful discussions on the photocurrent measurements with Dr. Chong-yang Liu and Professor Allen J. Bard.

Supplementary Material Available: Tables of bond lengths and angles and torsional angles for **1** (n = 7) (2 pages). This material is contained in libraries in microfiche, immediately follows this article in the microfilm version of the journal, and can be ordered from the ACS; see any current masthead page for ordering information.